RSC Advances

ROYAL SOCIETY OF CHEMISTRY

www.rsc.org/advances

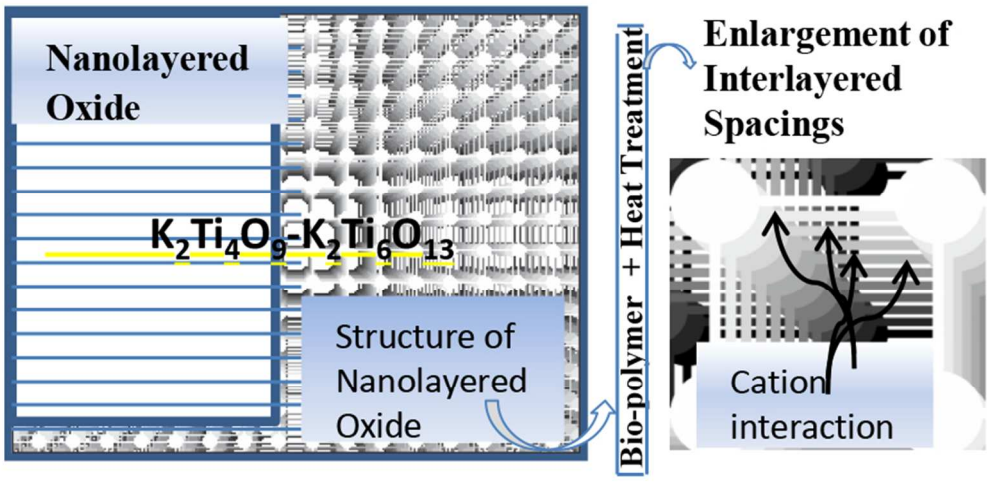

Polytitanates potassium are regarded as intelligent materials for their extraordinary properties of ion exchange among others and developing nanoframes, larger interlayered spacing are generated and therefore the activity of ion exchange is increased.
75x36mm (300 x 300 DPI)

RSC Advances RSCPublishing

ARTICLE

Potato starch: Binder and pore former in nanoframes of nanolayered oxides for Pb^{2+} and Ni^{2+} as pollutants in water and industrial sludge applications.

M. A. Aguilar González[a]*, A.A. Zaldivar Cadena[b], C. N. Aguilar[c], E. M. Múzquiz[d] and F. Equihua[e].

Received (in XXXX),XthXXXXXXX20xx, Accepted XthXXXXXXX20xx

DOI: xxxxx/xoxxoooooox

This article deals with the importance of the potato starch in two different applications, as a pore former and also as a binder in microporous/mesoporous ceramic adsorbents in order to remove toxic metal pollutants in water. These porous ceramic adsorbents with unique and high adsorption and ion exchange properties in addition to an intricate structure were obtained by mixing 50% of potassium polytitanates (PPT) and 50% of potato starch (PS). Cylindrical pieces were obtained through a typical extrusion process. Additionally, a heat treatment in different stages was applied to these cylinders and later they were crushed to 2-5 mm of size. The physicochemical behavior of the adsorbents was assessed before and after of the sintering process by different techniques: thermal analysis, chemical analysis, optical microscopy, SEM, TEM, XRD, BET, Mercury porosimetry, mechanical properties and physicochemical methods. Amounts of 5-50 weight percent of PS were applied with PPT in order to produce adsorbents with a properly configured structure. Results in mechanical properties and adsorption tests showed that adsorbents removed cations of lead and nickel from the solution excellently. PPT have a technological and academic importance attributed to they have not yet been studied in linked form. It is possible to reduce diseases in people from the five continents whit treatments of polluted waters with these materials and also is given a valorization of some sectors of potato.

1. Introduction

Potato starch has been well recognized as a binder and pore forming agent in ceramic microstructures.[1] Some studies have established typical and modern processing methods for ceramic materials bonded by starch.[2] The ceramic porous materials play a very important role in the field of new advanced materials with functional properties. The application of PS (Potato Starch) in industrial processes is very extensive and diverse: food,[3] paper,[4] diesel particle filters,[5] porous piezoelectric ceramics,[6] hydrogel composites,[7] anodes in fuel cells,[8] and clinical applications.[9]

Porous ceramic bodies formed with advanced nanomateriales of titanates have a great potential for many applications; however, they have not been utilized neither in the immobilization of toxic pollutants in water ions nor in metal coating sludge. In both cases, it seems as if having porous support with activated surface for more adsorption can enhance the efficiency of the applied material.

New potassium polytitanates (PPT) based ceramic oxides of potassium have taken a major and essential importance in the research field due to some reasons such as their unique structures and properties as: thermal, chemical, catalytic, mechanical, non-frictional, refractory, optical, adsorbent, biomimetic and of ion exchange.

In the last decade, several routes have been proposed to synthesize potassium titanates among which can be found: chemical, thermal, hydrothermal and modification of titanium precursors by reactions in a solid or liquid state.[10]

Recently, it was reported that the development of a new type of ceramic nanomaterials called "potassium polytitanates" (PPT) obtained by molten salts with a short heat treatment route.[11] PPT are inexpensive and easily handled in ceramic technology. Also, it does not pose health risks in handling due to their laminar morphology. Treated at temperatures from 900 to 1300° C they allow the formation and recrystallization of different potassium titanates, depending of their synthesis.

Molten salt processes are regarded as highly important to chemical technology. The main applications are: metallic alloy production,[12] batteries,[13] fuel cells,[14]

catalysis,[15] photocatalysts[16] and solar energy.[17] Molten salts are studied for different purposes through many different techniques. The chemical and thermodynamic considerations of binary or ternary systems in solutions of molten salts have been very well established.[18]

Nowadays PPT are considered as a kind of intelligent ceramic materials[19] due to their ion exchange, intercalation and adsorption properties in radionuclide and radioactive materials preventing damage to human health and the environment. It is important to consider that there exist some reports of other modified ceramic materials where ion exchange and metal removal properties are related. [20,21,22,23,24]

Potassium titanates are ceramic systems with very similar chemical composition but their properties are very different, especially when their obtaining process involves heat treatments. The extrusion method was chosen for this research because it is a process that provides directionality to fine powders of laminar nature and/or irregular shapes (such as PPT). Besides this, the advantages of extrusion include the ability to add sintering aids, low shrinkage and flaws can be eliminated by colloidal processing of the paste. In this research we apply the conventional extrusion that is the best method for granular production, straightforward and inexpensive.

There is no evidence in the literature of titanates being bonded to starch as to study their adsorption or catalysis applications. The difficulty to link titanates arises mainly through the manipulation of layered powders in a micro or nanometric scale.

Then the innovation of our work suggests the handling of the starch granules in ceramic pastes to a strict temperature of 50 °C. This treatment gives the maximum plasticity in order to form bodies in green (before sintering) and saving the application of chemical or organic binders (environmental contribution). It is well-known that the degree of swellability will depend on its uniformity in porosity. There are others important methods for making porous ceramic with starch and water such as consolidation (slip casting), gel casting or tape casting.

In this paper, we present important evidences about the application of PS as pore former and as a binder in microporous/mesoporous ceramic adsorbents to remove metallic toxic pollutants in water. Porous ceramics based on PPT linked through PS, extruded conventionally and heat treated were obtained and evaluated.

2. Experimental Procedure

2.1. PPT Preparation (as precursor materials)

PPT were prepared through molten salt synthesis. Analytical reagents (wt.% = 82-KNO_3, 8-KOH and 10-TiO_2, all with 99.7% of purity) were used to synthesize quasi-crystalline PPT according to previous work.[11] The obtained molten salts were heat treated at 500° C. Afterwards, dried TiO_2 powder (average= 0.4 μm) was added to a stainless steel crucible, during 1 hour in order to obtain PPT as precursor materials. Molten material was cooled to room temperature and then crushed. The ground material was thoroughly washed with distilled water and separated with a filter paper (No. 42). Powders were dried at 90 ° C during 2 hours.

2.2 Preparation of adsorbents.

Commercial grade of PS (73 amylose -27 amylopectine wt.%) was obtained from Sabritas® S.A de C.V (Saltillo Coahuila, México). PS was chosen according to a research with 5 different starches for ceramic applications[25] and the other reason was due to its negligible ash content after heat treatment (at least from the standpoint of materials science) compared with others organics. Potato starch was applied in natural form. The method for synthesizing of adsorbents is presented in Figure 1. It was reported that this route can yield the best volumetric expansion of the starch.[26]

2.3 Reagents and solutions.

Lead nitrate and nickel nitrate (Aldrich, 99% of purity) were used for absorption tests in aqueous solutions at a concentration of 155 mg/L in distilled water and pH values of 5.6 and 7.5 for lead and nickel respectively. These solutions were used directly in adsorption tests. Both solutions were used to investigate the amount of Pb (II) or Ni (II) removed in solutions as industrial wastes.[27]

2.4 Characterization

The density of the adsorbent materials was determined using the Archimedes principle, using Toluene of 99.5% purity. Measurements were made at 25 °C on an analytical balance (Ohaus, Explorer) according to ASTM C373-88 (2006). A BET surface area of 13.4 m^2/g and an average particle size of 35 microns for PPT were used as the starting materials. Brunauer-Emmet-Teller (BET) and analysis of micro-pores (MP) were selected in a Quantachrome Autosorb 1C sortometer using the adsorption/desorption technique of a monolayer of nitrogen. The average grain size for PS was of 64 μm determined through the Laser Coulter Technique. SEM analyses were made in a Scanning Electron Microscope Philips XL30, ESEM (Environmental Scanning Electron Microscope) equipped with EDS (Pegassus, operated at 20 kV of acceleration voltage). The identification of crystalline phases was performed by X-ray diffractometry in an X-ray Diffractometer by Philips X'Pert using Kα(Cu) radiation and a secondary monochromator (Ni filtering) at 40 kV and 30 mA. Thermal analysis was performed on a Perkin Elmer analyzer, model 1700. 10 mg of each sample was weighed and heated with a rate of 3 °C/min during overall analysis in the thermobalance.

Using two different methods, the porosity of the samples was evaluated: a) the novel ceramographic method, using the software: Image Pro Plus 5.1 (Media Cybernetics) for SEM images (BSE), and b) The Mercury intrusion porosimetry method. In the former, epoxy resin in presence of a vacuum was penetrated into the samples according to the ASTM E-3 standard. Then the metallographic surfaces were prepared and coated with gold. The porosity evaluation was performed with 20 different fields. In the latter, the samples were directly applied to the determining method. Mechanical properties of the porous ceramics were measured through the compressive strength with a hydraulic machine (Controls, Sercom 7) using a cell of 15kN and a loading rate of 100 N/s. 6 cylindrical samples were tested in each experiment.

Fact-Sage® software was used to calculate crystalline phases and possible transformations.

2.5 Adsorption Test.

2.5.1 Static and dynamic experiments - Adsorption Kinetics of Pb and Ni.

To observe the alkaline behavior (value close to 12) of the adsorbent in aqueous media, before the adsorption tests with metal ions, several experiments were assessed with double distilled water (90 V%) and PPT adsorbents (10 V%) in glass flasks with constant agitation at 120 r.p.m (24 hours for batch type tests) and room temperature.

In the static experiments, 2 grams of adsorbents were placed in 200 ml solutions. Different contact times (0, 7, 15, 30, 60, 120, 180, 240, 360 and 420 min) were considered for static adsorption tests.

For the dynamic mode a special pyrex glass device was used to feed fluid into a Pyrex® glass column (Diameter= 25mm) with the capacity of 500 cm^3 at 23 ±2 °C. Adsorbent pellets (165 g) which have occupied a third of the glass column were used during this experiment. The flow rate of the solution was kept constant at 140 ml/hour during 40 hours.

The adsorption kinetics of Pb (II) and Ni (II) present in their aqueous solutions were determined by the atomic emission spectrometer (ICP Thermojarrel Thermoelemental Ash, Iris Intrepid II model). The spectrometer was calibrated with NIST certified standards.

The metal concentration retained in the adsorbent phase (qe, mg/g) was calculated as follow:

$$qe = ((Co-Ce)/V)/m, \quad (1).$$

where: *Co* and *Ce* are the initial and final concentrations of the metal ion in solution (mg/L), *V* is the volume of solution (ml) and *m* is the mass of adsorbent (mg).

3. Results and discussion

3.1 Thermal Behavior

Chemical processes, properties and types of PS have been investigated in ceramic applications in order to understand structural and crystalline arrangements of each component of PS[28,29] and therefore the thermal behavior. It is well known that the PS granules are insoluble in water below 50 °C; in our work, a gelling temperature range from 55 and up to 80° C was present, as it can be seen in figure 2(a) for PS as a raw material. During the gelation stage, water absorption was limited due to the swelling of the starch particles, which increased their size several times in an irreversible process.[30]

We found that the gelatinization temperature for the PS granules mixed with PPT and water was about 65° C in a 50:50 W% relationship, respectively. While heating, wet pastes began to swell forming a highly viscous white paste.

On the first stage, the extruded samples were dried at 65°C during two hours, which was enough for swelling up the starch granules. In the temperature range from 25 to 140 ° C, PS showed two outcomes: 1) the loss in weight related to the evaporation of adsorbed water and 2) the endothermic effect with a more intense heat of 80° C. This process corresponds to volumetric expansion of the starch and hence the results in a gelation stage.[31] After that, the temperature was increased to 180 °C in order to evaporate water completely.

When the temperature was increased from 275 to 350° C, starch granules showed a weight loss of about 60%, which corresponds to thermal decomposition.[32] Then, to totally ensure the decomposition of PS in the extruded bodies a second stage of heat treatment at 500°C was selected. While burning the starch granules were calcinated in pyrodextrinization reactions[30] in order to make hollows in the ceramic bodies.

Figure 2a shows the representative graphs of the transformation of the potato starch, in the process of swelling as it gets into contact with water at a temperature range between 25 and 350° C, a similar behavior was studied by Laurentin and co-workers.[30] Furthermore, PPT adsorbed water (removed from 350 to 550 °C) and structural water (removed from 500 to 700° C) were detected, figure 2(b).The thermogram TG in figure 2(b) shows a partial weight loss of the sample, during the analysis of 9.8 (W%) at 714° C, generated by the decomposition of Ti-OH groups[33], which correspond to a removal of structural water. On the final stage, a small endothermic change was detected at 1050° C, due to the recrystallization and structural transformation that were present during the Ti phase formation.

Additionally, regarding the sintering process, one can say that the final products from starch will always be CO_2 and H_2O, as long as this is all performed in oxidizing atmosphere. Of course, under reducing conditions,

residual carbon may occur. The PS breakdown begins to be detected below 300° C. [30]

3.2 Morphology, microstructure and phase composition.

3.2.1 Starting Materials.

According to the SEM survey, figure 3(a) shows granules of PS as raw material with an ellipsoidal morphology and with an average size of 30 microns. These values are similar to those obtained in other studies for porous ceramic material synthesis.[34] Also, it was demonstrated by the SEM that the adsorbents contain transport pores with an average diameter of 35 microns, reported through mercury porosimetry intrusion, which is similar to the size of the particles of starch used as a raw material. Moreover, the PPT were constituted by aggregates of micrometric size, which have a composition of lamellar particles (plaques) with dimensions from 400 to 1000 nm and a plate thickness smaller than 100 nm, figure 3(b).

3.2.2 Green Stage and Sinter.

For the first time, this work has shown SEM microphotographs of the starch granules coated with ceramic material. This gives a clear idea of the stage in which pores were formed (figure 4(b)), condition in green). After the sintering process, cylindrical shapes were obtained and crushed figure 4(a) and figure 4(c). The adsorbents were applied as granular materials in two different ways: 1) as a similar shape to those for its industrial application in columns and 2) in static batch type experiments figure 4(c) and figure 4(d). Figure 4(e) shows a granular adsorbent mounted polished resin.
The advantage in granular material is that it allows for impurities or other pollutants in a fluid to be reversibly separated. The porosity was open and different morphologies were observed for PPT before and after sintering. By applying a granular adsorbent, it was prevented that the adsorbed particles were agglomerated at the bottom of the adsorption container; this was also reviewed through SEM.
The adsorbent material developed a network of pores (average diameter of 35 microns). The spaces left by PS in sintered structures of PPT favor an increase in the interlaminar spacing of the crystalline structure 2.3 nm figure 5(b) and where a significant amount of ion exchange had apparently occurred. Figure 5(a) shows agglomerates of irregular morphology such as $K_2Ti_4O_6$ (short fibers) and $K_2Ti_6O_{13}$ (needles) in synthesized powders at 500 °C with agglomerates of different sizes and morphologies.

3.3 XRD

3.3.1 PPT synthesized at 500 °C

PPT phases showed a quasi-crystalline nature for a K_20/TiO_2 value of 5.1. The main diffraction intensities in XRD analysis were obtained in the following angles 2θ of Bragg: 11.2, 23.9, 29.8, 33.1, 34.7, 37.8, 43.1, 47.5, 47.7, 51.9, 55.1, 57.3, 58.7, 59.2, 61.9 and 66.4° figure 6(a). With these data the phases were identified using the 2004 version of the ICDD database. Consequently, it was found that some types of mixed alkaline titanates (lepidocrocite) with a layered structure have an order of reflection very similar to that of the PPT corresponding to the identifications of: $K_{0.8}Li_{0.27}Ti_{1.73}O_4$, ICDD with number of card=01-089-5420; and $K_{0.8}Mg_{0.4}Ti_{1.6}O_4$, ICDD with a number of card 01-073-0671. Here, TiO_2 contents were also shown without reacting as an Anatase phase with card number 21-1272, figure 6(a).
The estimation of the anatase content in the produced PPT was similar to those realized by means of quantitative X-Ray analysis.[35] The treatment time allows that the anatase to fully transform into PPT. A survey of transformation of TiO_2 was realized by Wallenberg and co-workers. [39]

3.3.2 Potato Starch

The XRD diffractogram (b) in figure 6 shows a type B crystalline structure of starch, which corresponds to a natural structure of starch from a dilute solution.[36] This material was identified with the chart number: 00-39-1912 ($C_6H_{10}O_5$). The main diffraction intensities were recorded in 17.2, 19.5, 22.2 24, 26.3 and 34.4 ° 2θ Bragg degrees. For 6(c) a pattern of a ceramic green sample (extrusion stage), the identified phases were: $K_{0.80}Ti_{0.40}Mg_{1.60}O_4$ and potato starch. For the pattern 6(d) a sample heat treated at 1100° C (sintering) and was identified as $K_2Ti_6O_{13}$ phase. These samples belonged to the 50 PPT-50 SP (W %) system.
With all aforementioned data, it was determined that the PS was not involved in the process of recrystallization of PPT.

3.4 Porosity

Transport pores were promoted naturally through the extrusion and they confirmed their presence at the sintering stage. This favored the open porosity.
A portion of the generated porosity is considered a consequence of the recrystallization between acicular and tangled microstructures. When the ceramic bodies were formed, they generated spaces (internally), this allowed the growth and recrystallization of PPT and thus a structural rearrangement of potassium hexa-titanate, always in the presence of heat. Firstly, they had an irregular shape figure 3(b) which was converted to a fibrous form figure 7(f). Through mercury porosimetry it was observed that the starting adsorbent contained transport pores of 0.4 microns (35% of total porosity), macropores in a range from 0.05 to 0.4 microns in diameter as well as mesopores with diameters smaller

than 0.05 microns. Similar results were obtained by Ohta and Fujiki.[37] This means that there is no risk for health in the manipulation of fibers through the extrusion process (homogeneous and fluid pastes). The evaluation of total porosity in adsorbents was 63.7 % (optical) and 67% (SEM).

A research work on the factors that affect the morphology such as diameter, length and synthesis rate of potassium titanates was done by Zaremba et al.[33] But the most important physical aspect in PPT is that they allow the retention of the pollutants with interactions in their interlayer spacings.

3.5 Specific surface area.

The specific surface area values frequently are altered for various reasons, mainly due to the content of titanium.[39] PPT precursors showed an average value of 13.9 m^2/g when were analyzed through nitrogen adsorption which coincides with the research reported by Wallenberg and co-workers.[34] The BET values in the PPT were lower in comparison to commercial adsorbents.

The morphological characteristics such as: a non-porous particulate structure and an accordion-like shape can affect the exposed surface area of such materials. The PPT-PS ceramic adsorbents (sintered) obtained an average value of specific surface area that was of 0.65 m^2/g. The specific surface area of the sintered materials was lower than the synthesized ones; this can be attributed to the recrystallization through heat treatment effects and thus presenting an exchange in their morphology.[39] This report allowed us to observe irregular agglomerated materials figure 3(b) such as raw materials and later converted to intricate beams with an acicular morphology which were obtained after the heat treatment figure 7(e) and figure 7 (f). Whereas the exhausted adsorbent showed an average value of 1.2 m^2/g.

3.6 Mechanical Properties.

The best mechanical properties were presented in the 50:50 PPT-PS system (3.2 of density) and they were enough for rough handling of the materials in green. PS acted as a binder and pore former in the obtained porous ceramic material, favoring a high mechanical strength on the order of 103 MPa. The mechanical strength for filters/adsorbents must possess a value around 100 MPa according to the application of each material.[40]

Heat treatment generated an intricately interconnected structure in the adsorbent promoted by the use of PS granules. This structure improved the mechanical properties compared to the PPT without mixing Fig. 7(a) and also prevented the effect of clogging. These were all the results for the green condition: 14.57, 22.92, 34-62, 47.63 and 61.83 MPa and 48.62, 59.14, 70.27, 84.99 and 103.70 MPa, in sintered samples, for 10, 20, 30 40 and 50 % PS respectively. The worst results were attributed to the system with 10% of PS.

3.7 Adsorption Kinetics

3.7.1 Dynamic adsorption of Lead.

All experiments were performed independently. Figure 8a (black triangles down) shows the effect of the Pb^{2+} ions concentration as a function of contact time with the adsorbent where a high efficiency of removal of lead ions in solution was observed (initial solution with pH=5.6). The greater effectiveness of removal was observed in the first three hours of contact time which decreased of 155 to 4.76 mg/L. The reactions that explain this behavior correspond to the equations (2) and (3). Meanwhile, during removal of lead, eluted solution (purified) showed a high content of K^+ ions, the concentration changed over time of the adsorbent saturation. In the first ten hours, potassium content increased from 0.07 to 104 mg/L and then was gradually increased until to 124.1 mg/dm^3 when the process was finished (Figure 8a, black triangles up). After passing the solution through the column completely, the initial concentration of lead ions decreased to 0.6 mg/L, this amount is according with the Land Disposal Restrictions for Third Scheduled Wastes" 55 FR 22520, EPA, USA, 1990. The concentration of K in the eluted solution can be explained by the presence of two ion exchange parallel processes as is present in the equations (1) and (5). With the increase of the K content of the eluted solution pH up to 10.6. The elution rate retained its initial value for 15 contact hours under constant hydrostatic pressure, and then decreased gradually of 140 to 100 cm^3/h (40 contact hours). The initial pH of the solution for the case of lead was set at a 5.6, this was agreed to several experiments previously conducted and also according to reports in the literature for the lead ion electrochemistry. [27]

3.7.2 Dynamic adsorption of Nickel.

Figure 8a, (white triangles down) illustrates the removal of nickel ions in solution (initial pH=7.5), where the initial concentration decreased of 155 to 0.6 mg/L in the first three hours of time of contact time (maximum efficiency of removal). After that, the concentration of Ni^{2+} decreased gradually until the end of process and reached 0.1 mg/L. Moreover, during the process, the eluted solution (purified) showed a high content of K^+, therefore the concentration changed over time of the adsorbent saturation. Simultaneously, in the first five hours, potassium content was increased from 0.05 to 50 mg/L and then to the end of the process, this ion increased its value to 114 mg/L, Figure 8a (white triangles up). Adsorption mechanisms were attributed to the equations (2) and (3) and for the increment of potassium to the equation (5).

The initial pH of the solution for the case of nickel was set at a 7.5, this was agreed to several experiments previously conducted and also according to reports in the literature for the nickel ion electrochemistry.[27]

3.7.3 Static adsorption of Lead.

Figure 8b (black triangles down) shows the graph for the adsorption of lead ions which was carried out with porous ceramic adsorbents based potassium polytitanates with a solution containing 155 mg/L of lead. A decrease in the lead concentration was observed after of the first hour of the contact time with a value of 36 mg/L. This amount represents 76.77 % of the total removal, the rest was performed after the first hour and to the end of the process and for contact times of 3 h or higher the changes in lead concentration for the aqueous solution were minimal. During the process, potassium ions were released into the solution and simultaneously increased in accordance to the decrement of Pb content. At the end of the process the amount of potassium present in solution reached the value of 96 mg/L, Figure 8b (black triangles up).

Maximum amount removed of lead ions by the adsorbent was 28.8 mg/g at 5.6 of pH value and with 99.94% of total effectiveness of removal. This allowed us to propose that the adsorption may have occurred by ion exchange explained by equations (2) and (3).

3.7.4 Static adsorption of Nickel.

Figure 8b(white triangles down) shows a statically adsorbed nickel plot. The rate of removal of nickel in this mode proved to be the slowest of all experimental series conducted; it represents 54% of the total adsorption (first hour). In parallel an increase of 59.3 % of concentration of potassium ions was observed at the same time, Figure 8b(white triangles up). A value of 71.69 mg/L was registered during the first hour. The content of nickel in solution at the end of the process was 0.12 mg/L. The remained content of nickel is within the specified for industrial wastewater discharge. In this stage the maximum amount removed for nickel ions was 19.9 mg/g of adsorbent. At 7.5 of pH value and with 99.7% of effectiveness. In the case of potassium ions in solution a trend of steady increase was always observed.

The main reactions for metal ions may ocurr as follow:

$$Me^{2+}_{(solution)} + H_2O \leftrightarrow MeOH^{+}_{(solution)} + H^{+}_{(solution)} \quad (2)$$

$$MeOH^{+}_{(solution)} + H_2O \leftrightarrow Me(OH)_{2(solution)} + H^{+}_{(solution)} \quad (3)$$

And the metal ion exchange could be as follow:

$$H^{+}_{(solution)} + Me^{+}_{(adsorbent)} \leftrightarrow H^{+}_{(adsorbent)} + Me^{+}_{(solution)} \quad (4)$$

$$Me^{2+}_{(solution)} + K^{+}_{(adsorbent)} \leftrightarrow Me^{2+}_{(adsorbent)} + 2K^{+}_{(solution)} \quad (5)$$

The adsorbents showed high effectiveness of adsorption for both Pb ions and Ni ions and after 15 minutes of contact time, concentrations were reduced to 0.1 mg/dm^3 in both cases, which are allowable levels according to standard EPA 55 FR 22520, 1990, USA. During the process, potassium ions were released into the solution and simultaneously increased in accordance to the decrement of metal content. This allowed us to propose that the adsorption may have occurred by ion exchange between Me^{2+} (solution) and K^{+} cations (of the adsorbent structure).

The fibers of PPT are considered different and unique morphologies since their materials underwent one crystalline transformation in a single direction.

The PPT absorbent capability of trapping hazardous cations permanently allowed us to isolate them from contaminated water. When the used adsorbents become saturated they can be confined safely without the risk of releasing the absorbed cations (through leaching effects).

The features of the adsorbents applied in this work such as: porosity, particle size, density, surface area, pore size and mechanical properties are consistent with those in the publications of Heckmann and Wenger and Harada and co-workers.[40,41]. The concentration of metal ions in solution used in this research of 155 mg/L was selected according to previous studies for adsorption of metal ions in solution.[42,43,44]

Acknowledgements

The authors would like to thank the CONACyT (México) for economic support to the realization of this research and M.Sc. Enrique Diaz Barriga for the support of the TEM Characterization.

4. Conclusions

The materials were obtained from extruded pastes whose composition was: 50% PPT with molar ratio TiO_2/K_2O=5.1 and 50% potato starch and distilled water (60 W% relative to the weight of solids), the materials were sintered at 1100° C during 30 minutes and were used as ceramic adsorbents. The crystalline phases occurred in the composition of potassium titanates and a structure similar to that of $K_2Ti_6O_{12}$. This structure is formed during heat treatment by a chemical reaction among PPT favoring high mechanical strength (about 110 MPa). The adsorbent material has developed a network of transportation pores (average diameter of 35 microns). The PPT favor increased interlayer spacing in a crystalline structure of up to 2.3 nm. As a result, the material showed a high rate of adsorption of lead and

nickel through an ion exchange mechanism with potassium incorporated into the structure of the adsorbents.

References

1 Z. Živcová, M. Černý, W. Pabst and E. Gregorová, *J. Eur. Ceram. Soc.,* 2009, 29, 2765-2771.
2 M. E. Gomes, A. S. Ribeiro, P. B. Malafaya, R. L. Reis and A. Cunha, *Biomaterials.,* 2001, 22, 883-889.
3 A. Cheyne, J. Barnes and D. I. Wilson, *J. Food Eng.*, 2005, 66, 1-12.
4 S. Jobling, *Curr. Opin. Plant Biol.,* 2004, 7, 210-218.
5 T. Wolff and H. Friedrich, GE Patent # 029481A1, 2011.
6 A. N. Rybyanates, *Ferroelectrics.,* 2011, 419, 90-96.
7 M. R. Guilherme, R. S. Oliveira, M. R. Mauricio, T. S. Cellet, G. M. Pereira, M. H. Kunita, E. C. Muniz and A. F. Rubira *Soft Matter.*, 2012, 8, 6629-6637.
8 A. Sanson, P. Pinasco and E. Roncari, *J. Eur. Ceram. Soc.,* 2008, 28, 1221-1226.
9 F. Romero and M. J. Bernal, *Starch/Stärke.,* 2011, 00, 1-11.
10 T. Zaremba and D. Witkowsca, *Mat. Sci. Pol.*, 2010, 28 25-
11 M. A. Aguilar, A. Gorokhovsky, A. Aguilar and J. I. Escalante, *Bol. Soc. Esp. Ceram.*, 2008, 47, 29-34.
12 M. Harata, K. Yasuda, H. Yakushiji and T. H. Okabe, *J. Alloys Compd.*, 2009, 474, 124-130.
13 Jp. Pat., WO2011148864A1A, 2011.
14 US. Pat., 2012021328A1, 2012.
15 Q. Wang, Z. Guo and J. S. Chung, *Mat. Res. Bull.,* 2009, 44 1973-1977.
16 T. Docters, J. M. Chovelon, J. M. Herrmann and J. P. Deloume *Appl. Cat. B: Environ.,* 2004, 50, 219-226.
17 US. Pat., 20120026495, 2012.
18 M. Blander, in: *Molten Salts Chemistry* An *introduction and selected applications*, Eds. G. Mamantov, R. Marassi, NATO Series C Mathematical and Physical Sciences, D. Reidel Publishing Company, Dordrecht, Holland, 1987, vol. 1, ch. 22, pp. 17-45.
19 D. J. Yang, Z. F. Zheng, H. Zhu, H. W. Liu and X. P. Gao *Adv. Mater.*, 2008, 20, 2777-2781.
20 F. Akhtar, L. Andersson, S. Ogunwumi, N. Hedin and L. Bergström, *J. Eur. Ceram. Soc.,* 2014, 34, 1643-1666.
21 R. Chen, Z. Zhang, Z. Lei, N. Sugiura*, Desalination.,* 2012, 286, 56-62.
22 S. Chattopahyay, US Patent # 0306555, 2014.
23 Y.T. Fang, T. Liu, Z.C. Zhang, X.N. Gao, *Renewable Energy.*, 2014, 63, 755-761.
24 Y. Fang, W. Yao, J. Guo, and X. Gao, *International Journal of Low-Carbon Technologies.,* 2012, 0, 1-4.
25 E. Gregorová, W. Pabst and I. Boacenko, *J. Eur. Ceram. Soc.,* 2006, 26, 1301-1309.
26 M. H. Talou, M.A Villar and M. A. Camerucci, *Ceram. Int*., 2010, 36, 1017-1026.
27 J. G. Dean, F. L. Bosqui, and K. H. Lanouette, *Env. Sci. Tech*., 1972, 6, 518-524
28 E. Gregorová, Z. Zivcová and W. Pabst, *Starch/Stärke.,* 2009, 61, 495-
29 A. Kraak, *Ind. Crops Prod.*, 1993, 1, 107-112.
30 A. Laurentin, M. Cardenas , J. Ruales, E. Pérez and J. Tovar *J. Agric. Food Chem*., 2003, 51, 5510-5515.
31 L. Kroh , W. Jalyshko and J. Haseler, *Starch/Stärke,* 1996, 48, 426-433.
32 C. Mestres, F. Matencio, B. Pons , M. Yajid and G. Fliedel *Starch/ Stärke*, 1996, 48, 2-6.
33 A. V. Gorokhovsky, J. I. Escalante, T. Sánchez and C.A. Gutiérrez, *J. Eur. Ceram*. Soc., 2004, 24, 3541-3546.
34 E. Gregorová and W. Pabst, *J. Eur. Ceram. Soc.*, 2008, 27 669-672.
35 T. Sanchez, A. Gorokhovsky and J. I. Escalante, *J. Am. Ceram. Soc.*, 2008, 91, 3058-3065.
36 Å Rindlav-Westling, M. Stading and P. Gatenholm, *Blends Biomacromolecules*, 2002, 3, 84-91.
37 N. Ohta and Y. Fujiki *J. Ceram. Soc. Jpn., 1980,* 88, 1-10.
38 T. Zaremba, *Mat. Sci. Pol.,* 2012, 30, 180-188.
39 L. Wallenberg, M. Sanati and A. Andersson, *Microsc. Microanal. Microstruct.,* 1990, 1, 357-364.
40 US, Pat., 006737376B1, 2004.
41 M. Harada, T. Sasaki , Y. Ebina and M. Watanabe, *J. Photochem. and Photobiol. A Chem., 2002*, 148, 273-276.
42 M. Sobh, M. Moussawi, W. Rammal, A. Hijazi, H. Rammal, M. Reda, J. Toufaily and T. Hamieh, *American Journal of Phytomedicine and Clinical Therapeutics.*, 2014, 2, 1070-1080.
43 T. Yin, X. Huang, *Advanced Materials Research.,* 2014, 955, 2747-2750.
44 V.K. Gupta and A. Rastogi, *J. Hazard Mater.,* 2008, 152, 407-414.

[a] Center for Research and Advanced Studies of the National Polytechnic Institute (CINVESTAV-IPN). Avenida Industria Metalúrgica # 1062 Parque Industrial Saltillo-Ramos Arizpe, Ramos Arizpe, Coahuila, México. C.P- 25900. *corresponding author: mgzlz@hotmail.com; miguel.aguilar@cinvestav.edu.mx.
[b] Institute of Civil Engineering, Universidad Autónoma de Nuevo León, Av. Fidel Velásquez y Av. Universidad S/N Cd. Universitaria, San Nicolás de los Garza, Nuevo León 66451 México.
[c] Department of Food Science and Technology, School of Chemistry. Universidad Autónoma de Coahuila, Unidad Saltillo, 25 000. Saltillo, Coahuila, México.
[d] Department of Ceramic Materials, School of Chemistry. Universidad Autónoma de Coahuila, Unidad Saltillo, 25 280. Saltillo, Coahuila, México.
[e] Faculty of Mechanical and Electronic Engineering. Universidad Autónoma de Coahuila. Av. Barranquilla s/n, Colonia Guadalupe., Monclova, Coahuila, México. C.P. 25750.

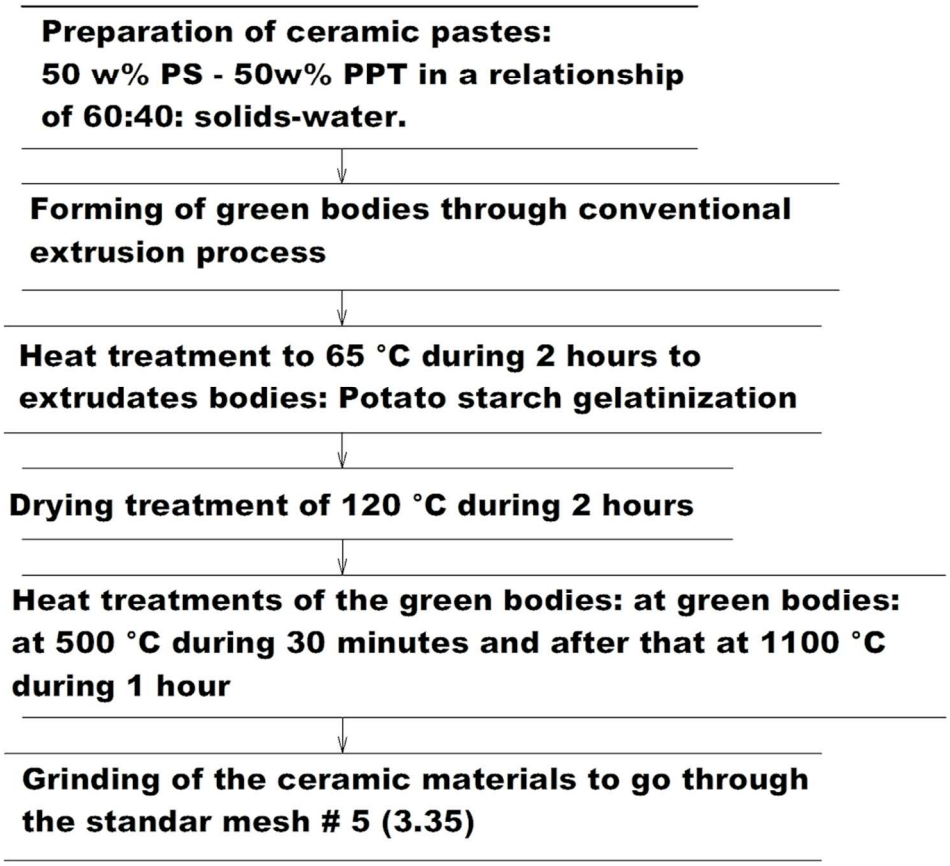

Figure 1. Flowchart for the making process of granular ceramic adsorbents.

99x102mm (300 x 300 DPI)

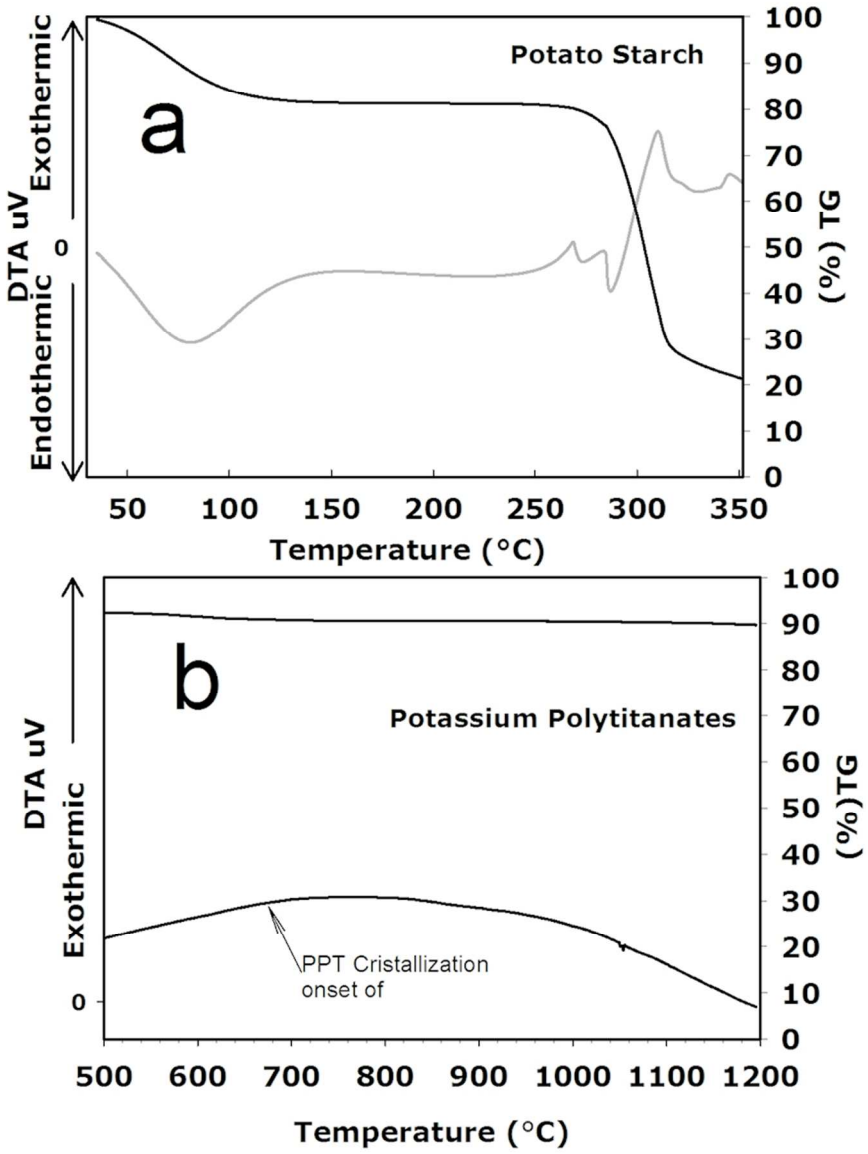

Figure 2.Thermal analisis for raw materials a) SP and b) PPT.
75x103mm (300 x 300 DPI)

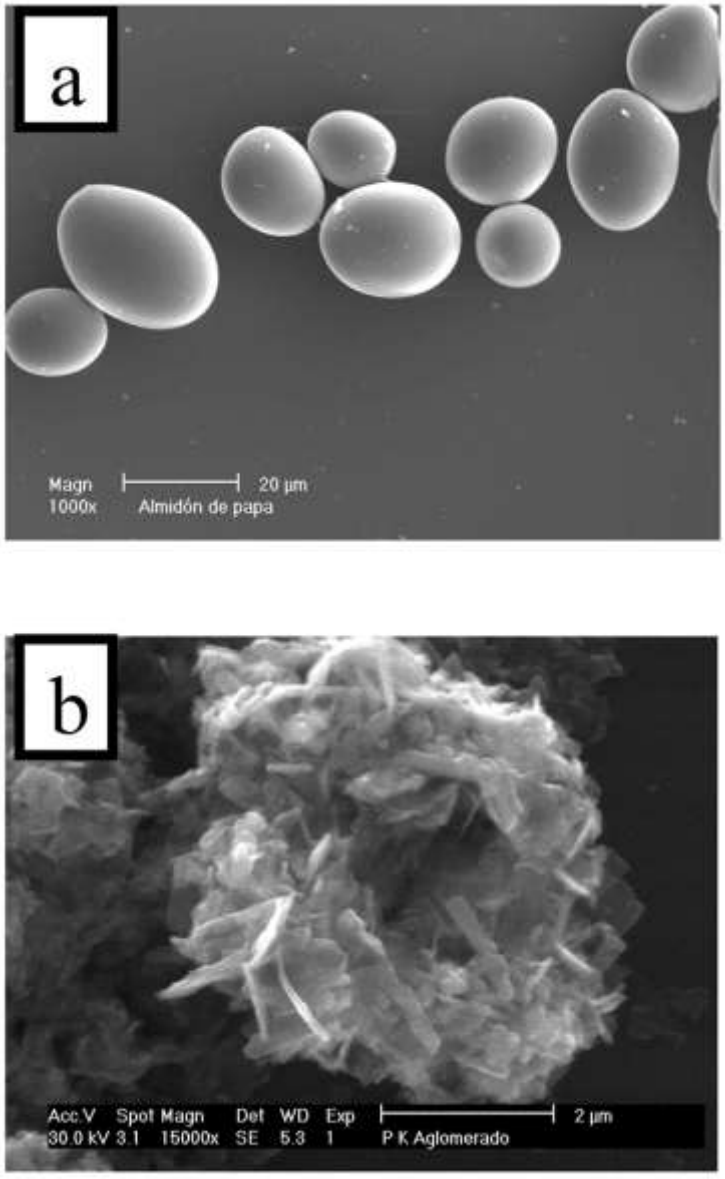

Figure 3. SEM images of start materials: a) starch potato and b) potassium polytitanates.
60x97mm (300 x 300 DPI)

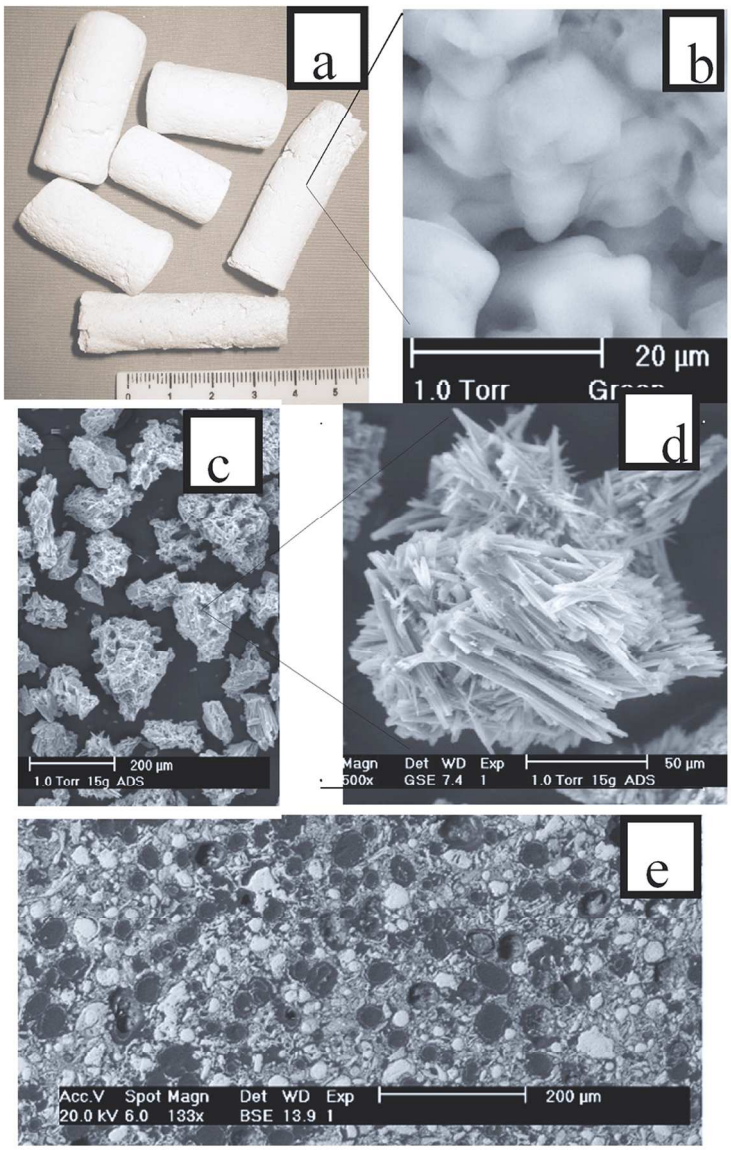

Figure 4. a) Stereoscopic microscope image: extruded in green, and SEM images: b) in green 1000X, c) granular 100X, d) granular 500 X and e) Cross Section in green mounted and polished.
90x141mm (300 x 300 DPI)

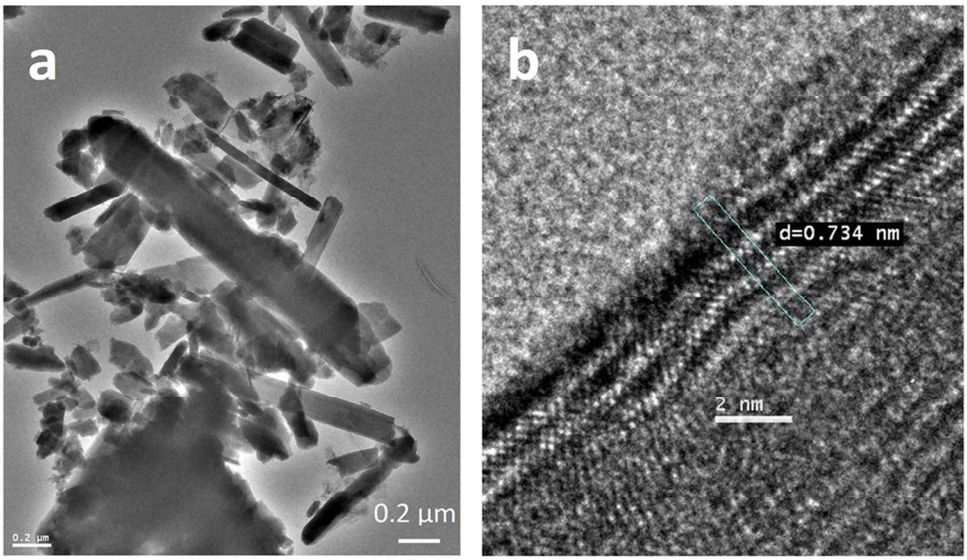

Figure 5. TEM micrographs a) PPT agglomerates synthesized powders to 500 °C. 50,000 X and b) Interlayer spacings inside of a PPT, sinter particle. 1,000 000 X.
99x60mm (300 x 300 DPI)

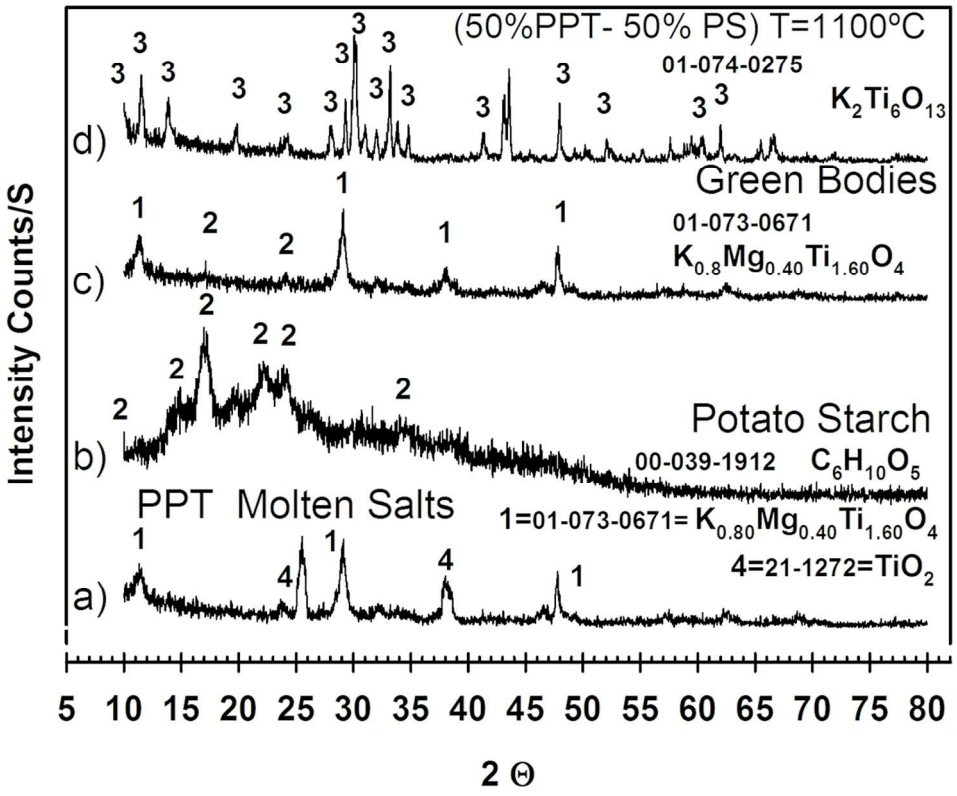

Figure 6. XRD patterns from: a)PPT synthesized at 500° C, b)potato starch, c) extruded sample 50SP-50PPT (W %) in green condition and d) 50SP-50PPT (W %) in sintered stage.
119x100mm (300 x 300 DPI)

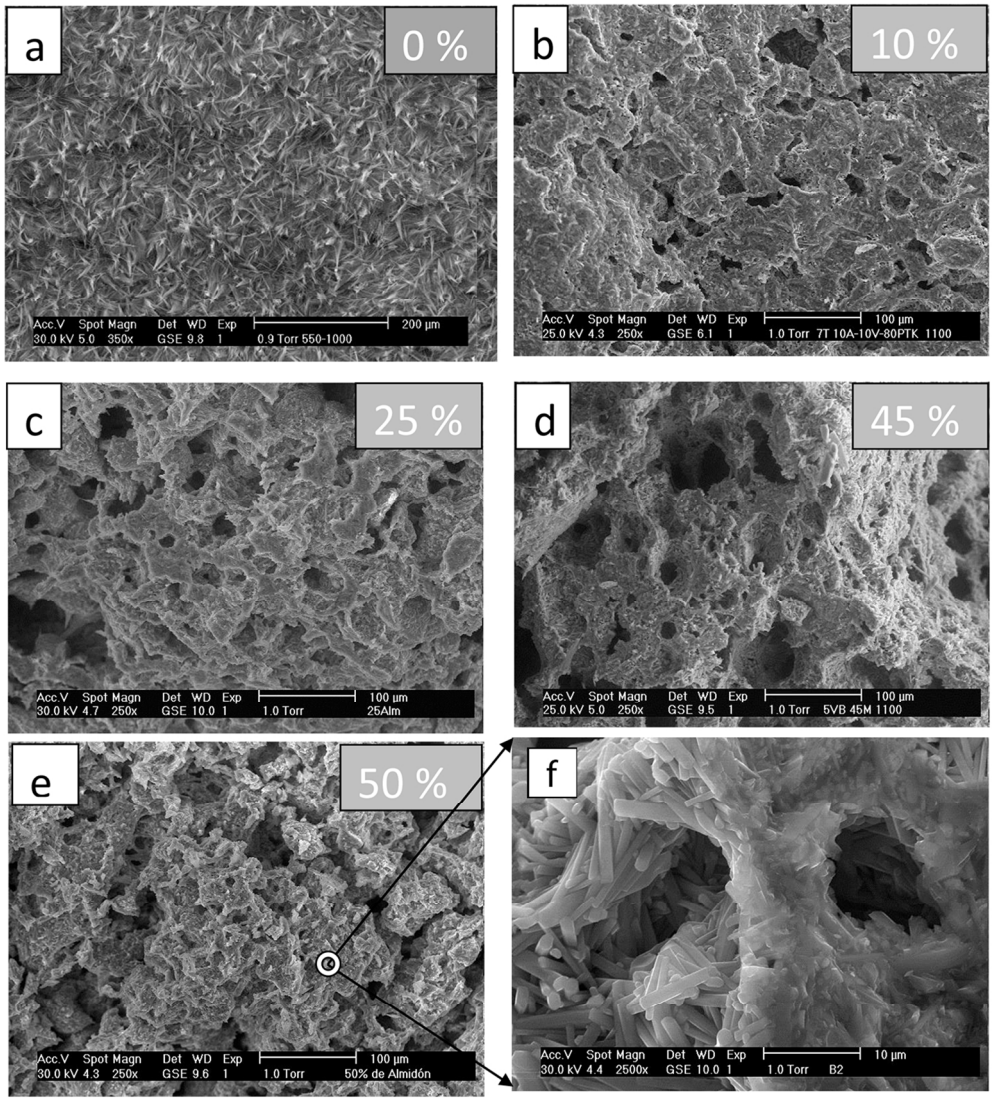

Figure 7. SEM photomicrographies of samples of adsorbent with different PS content: a)0%, b)10%, c)25%, d)45, e)50% and f) same that e) with 2500 X.
119x132mm (300 x 300 DPI)

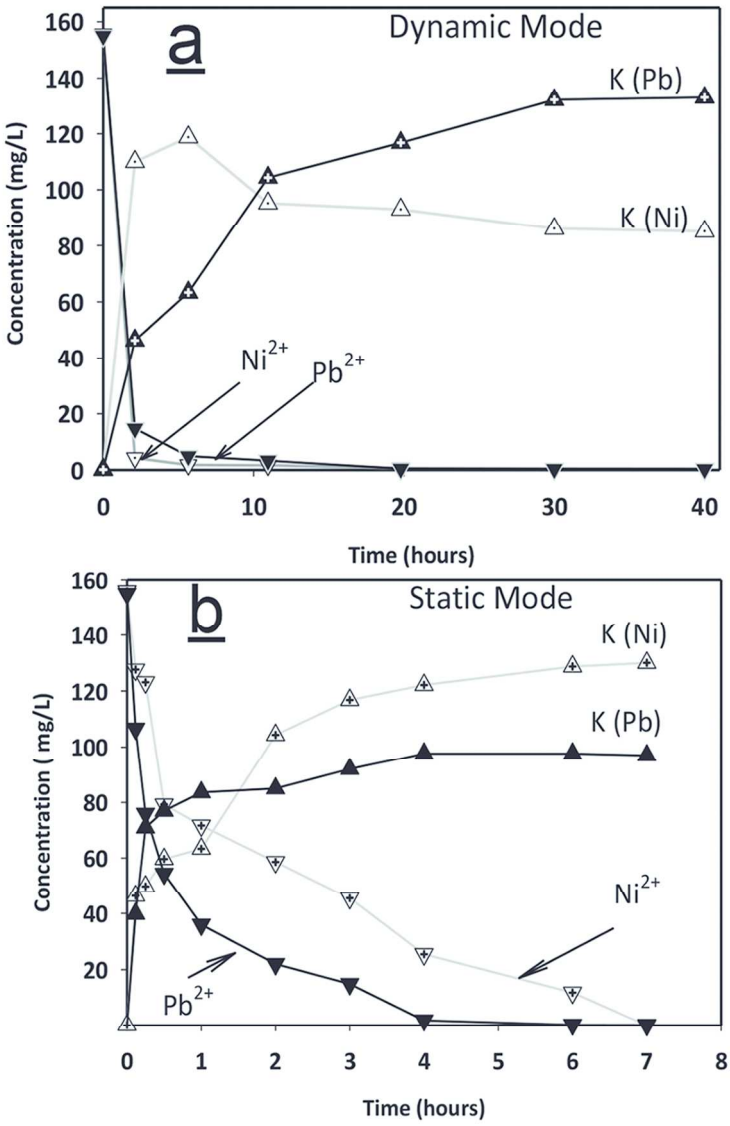

Figure 8. Kinetics of the removal of lead and nickel by adsorbents for: a)static mode and b) dynamic mode.

90x140mm (300 x 300 DPI)